

# Local Buckling Behavior of All-Steel Buckling Restrained Braces

**Nader, Hoveidae**

*Ph.D. Candidate, Faculty of Civil engineering, Sahand University of Technology, Sahand, Tabriz, East Azarbayjan, Iran*

**Behzad, Rafezy**

*Associate Professor, Faculty of Civil engineering, Sahand University of Technology, Sahand, Tabriz, East Azarbayjan, Iran*



## SUMMARY

This study presents the finite element analysis results of the proposed all-steel buckling restrained brace (BRB) models. The objective of the analyses is to conduct a parametric study to investigate the effect of interface detail of BRBs on local buckling behavior of the core plate. Moreover, the effects of magnitude of friction coefficient ( $\mu$ ) between the core and the buckling restraining mechanism (BRM) contact, the size of gap between the core and the BRM, and the unbonding material thickness on local buckling behavior of BRBs are investigated through the finite element analysis method. Based on the results, the interface configuration and the magnitude of friction coefficient at the interface could significantly affect the local buckling behavior of all-steel BRBs. Finally, an appropriate interface detail of BRBs is suggested for design purposes based on the finite element analyses results.

**Keywords:** *All-steel buckling restrained brace; Interface detail; Frictional response; local buckling; Finite element analysis.*

## 1. INTRODUCTION

Buckling restrained braced frames (BRBFs) for seismic load resistance have been widely used in recent years. A BRB differs from a conventional brace element because it yields under both tension and compression without significant buckling. Most buckling restrained brace (BRB) members currently available are built by inserting a steel plate into a steel tube filled with mortar or concrete. The steel plate is restrained laterally by the mortar or the steel tube and can yield in compression as well as tension, which results in comparable yield resistance and ductility, as well as a stable hysteretic behavior in BRBs. A Large body of knowledge exists on conventional BRBs' performance in the literature. Black et al. (2002) performed component testing of BRBs and modeled a hysteretic curve to compare the test results and found that the hysteretic curve of a BRB is stable, symmetrical, and ample. Inoue et al. (2001) introduced buckling restrained braces as hysteretic dampers to enhance the seismic response of building structures.

As shown in Fig. 1a, a typical BRB member consists of a steel core, a buckling restraining mechanism (BRM), and a separation gap or unbonding agent, allowing independent axial deformation of the inner core relative to the BRM. In addition, a detailed cross section of a typical all-steel BRB is represented in Fig. 1b.

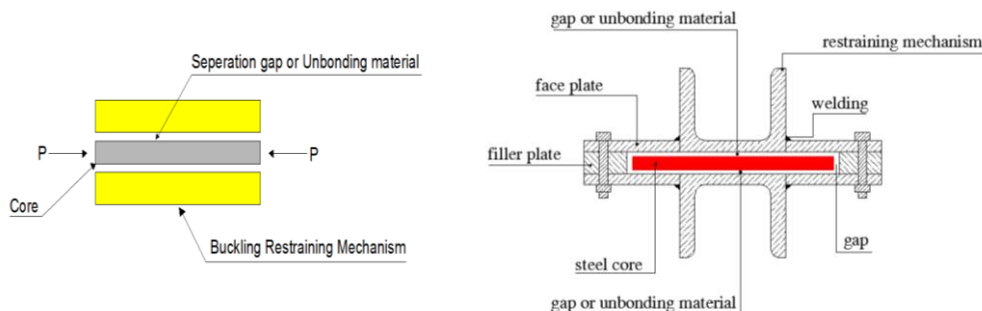


**Figure1.** a) Components of a BRB ; b) Typical Cross section of an all-steel BRB

Numerous researchers have conducted experiments and numerical analyses on BRBs for their incorporation into seismic force resisting systems. Qiang (2005) investigated the use of BRBs for practical applications for buildings in Asia. Clark et al. (1999) suggested a design procedure for buildings incorporating BRBs. Sabelli et al. (2003) reported seismic demands on BRBs through a seismic response analysis of BRB frames. Fahnstock et al. (2007) conducted a numerical analysis and pseudo dynamic experiments of large-scale BRB frames in the US.

Local buckling behavior of BRBs has been studied by Takeuchi et al. (2005). Similar experimental tests were conducted by Wei et al. (2008) to survey the local buckling behavior of BRBs. The effective buckling load of BRBs considering the stiffness of the end connection was recently studied by Tembata et al. (2004) and Kinoshita et al. (2007).

Previous studies have demonstrated the potential of manufacturing BRB systems made entirely of steel, called all-steel BRBs (Tremblay et al. 2006). In a common all-steel BRB, the steel inner core is sandwiched between a buckling restraining mechanism made entirely of steel components, thus avoiding the costs of the mortar needed in conventional BRBs. This eliminates the fabrication steps associated with pouring and curing the mortar or concrete, significantly reducing manufacturing time and costs. In addition, such a BRB can be easily disassembled for inspection after an earthquake.

Experimental and analytical studies on deformation performance and dynamic response of BRBs have been performed by Kato et al. (2002), Watanabe et al. (2003), and Usami et al. (2006). The restraining member proposed previously was a mortar-filled steel section, which made an extremely rigid member. In such types of BRBs, the brace member and the BRM were integrated, and overall buckling did not occur. However, in all-steel BRBs, the brace member is made completely of steel, and the BRM system is lighter in comparison to conventional BRBs, which leads to a high potential for brace overall buckling caused by the low rigidity and stiffness of the BRM. The hysteretic behavior of all-steel BRBs was experimentally investigated by Tremblay et al. (2006). An experimental study on the hysteretic behavior of all-steel BRBs was also conducted by Eryasar et al. (2010). Analytical simulations and experimental tests on BRBs were conducted by Chou et al. (2010) to investigate the effect of restraining member size, number of bolts connecting the BRM components, core length, and cross sectional area of the core plates in BRBs.

The Finite element analysis method was recently used with success to predict the buckling response of the core plate in BRBs with tubes filled with mortar (Matsui et al. 2008). Subsequent numerical studies have been conducted by korrzekwa et al. (2009) to investigate local buckling behavior of the core plate in all-steel BRBs, which provided a description of the complex interaction that develops between the brace core and the BRM. In the mentioned studies, Outward forces induced by the contact forces were found to be resisted in flexure by the BRM components. Moreover, the contact forces resulted in longitudinal frictional forces that induced axial compression loads in the BRM.

In another experimental work, Ma et al. (2008) conducted experimental tests on six all-steel BRBs and studied the hysteretic behavior of the braces. A significant amount of research work has been performed in Japan and elsewhere in Asia over the last few decades for the development of BRBs (Xie 2005). A detailed summary of findings are epitomized in a report by Uang et al. (2004).

Most of BRB members are proprietary, but their concepts are essentially similar (Nakamura et al. 2000). Preparatory BRBs that have been developed in Japan are trended as hysteretic dampers in design, and no design provisions are available (Uang et al. 2004). In the United States, however, design recommendations have recently been incorporated into AISC 341-05 seismic provisions for structural steel buildings. This provision requires qualifying cyclic tests to be performed on a sub-assembly and uniaxial tests specimen. For the design of bracing and adjoining members, AISC 341-05 specifications require the use of adjusted brace strength ( $P_{abs}$ ), which is defined as follows:

$$\text{In compression: } P_{abs} = \beta \omega P_{ysc} \quad (1)$$

In tension: 
$$P_{abs} = \omega P_{y_{sc}} \quad (2)$$

$$P_{y_{sc}} = F_{y_{sc}} A_{sc} \quad (3)$$

where  $F_{y_{sc}}$  is the actual yield stress of the steel core as determined from a coupon test,  $A_{sc}$  is the net area of the core,  $\beta$  is the compression strength adjustment factor, and  $\omega$  is the strain hardening adjustment factor. The adjustment factors  $\beta$  and  $\omega$ , which are solely dependent on BRB details, usually are determined by testing. When subjected to a strong ground motions, a BRB member can sustain axial strains that are 10 to 20 times their yield strains. During any inelastic excursion, cyclic hardening of the core material takes place, which enhances the brace force beyond the yield force,  $P_{y_{sc}}$ . Furthermore, due to manufacturing details, certain amount of friction that develops between the core and the BRM is inevitable. Transfer of frictional forces also results in an increase in the brace axial force. The strain hardening adjustment factor,  $\omega$ , is calculated as the ratio of the maximum tension force to the yield force,  $P_{y_{sc}}$ . When a BRB is subjected to compression, lateral expansion of the steel core occurs due to the Poisson's effect. The area of the steel core and frictional resistance due to contact between the core and the BRM increase due to the lateral expansion of the core. Because of the Poisson's effect and frictional response, compressive force level attained is higher than the tensile load level for the same axial displacement demand. The compression strength adjustment factor,  $\beta$ , is calculated as the ratio of the maximum compression force to the maximum tension force of the brace. AISC seismic provisions mandates that the compression strength adjustment factor,  $\beta$ , be less than 1.3.

Despite of existing enough studies on conventional BRBs, the behavior of all-steel BRBs has not largely been studied in detail. In a recent study by Tremblay et al. (2006 and 2009); the authors concluded that all-steel BRBs have potential for adequate ductile seismic response. However, their tests results revealed the necessity to control the local buckling response of the core to minimize frictional response between the core and the BRM and develop a closely uniform strain demand in the core plate. Moreover, authors concluded that further research is required to study the effect of unbonding material on the brace local and global responses. Based on the discussion above, it is apparent that the performance of all-steel BRBs is limited due to the problems associated with the core and BRM interaction. In this paper, the finite element analysis method is employed to investigate local buckling behavior of all-steel BRBs. The analyses consist of three parts. In the first section, the effect of core and BRM interface configuration on local buckling behavior of the brace is investigated. In the second part, the influence of the magnitude of friction coefficient,  $\mu$ , between the core and the BRM contact surface on local buckling behavior of the core plate is examined, and in the last part, the effect of the size of the gap or unbonding material thickness is surveyed.

## 2. DESCRIPTION OF THE MODELS

The analyses consist of two parts. In the first part, local buckling behavior of the models S1g0c1, S1g1c1, and S1u1 are investigated regarding various types of the core and the BRM interface details. Three types of interface configurations are considered in this section. First, the direct contact between the core and the BRM, i.e., the model S1g0c1, second, using gap with the size of 1mm through the core thickness, i.e., the model S1g1c1, and the third, the model S1u1 containing unbonding material with the thickness of 1mm in both upper and lower sides of the core plate. In addition, a constant 2mm gap is considered through the core width in all of the models to allow for free expansion of the core plate about the strong axis. BRB models' specifications and geometries are summarized in Table 1. Regarding the studies in the field (Chou et al. 2010), a coefficient of friction of 0.1 was adopted to provide a greasy interface between the core and the BRM.

In the second part of the analyses, eight BRBs consist of the models S1g0c1, S1g0c2, S2g0c1, S2g0c2, S1g1c1, S1g1c2, S2g1c1, and S2g1c2 are considered to survey the effect of the magnitude of friction coefficient,  $\mu$ , between the core and the BRM on local buckling performance of the brace. Table 1 summarizes the models' properties.

All of the models consist of a constant  $10 \times 1 \text{ cm}^2$  core plate with various cross section types for the BRM members. The total length of the BRBs,  $L$ , is assumed to be 200 cm. The core plate and the BRM are modeled using 8-node C3D8 brick elements. Large displacement static cyclic analysis is performed using the ABAQUS 6.9.3 general-purpose finite element program. The core plate is expected to undergo large inelastic deformations and higher mode buckling with pronounced curvature. Therefore, a refined mesh is adopted with five elements across the plate and two over the thickness. A coarser mesh is used for the BRM because most of this component is expected to remain elastic. Contact properties with hard stiffness in the transverse direction and tangential coulomb frictional behavior are assumed between the core and the BRM elements. The contact model allows for the separation of the core plate from the BRM element, which enables the higher mode buckling of the core plate. The core plate and the BRM components are made of steel with a yield stress of  $F_y = 3700 \text{ Kg/cm}^2$ . A young module of  $2 \times 10^6 \text{ Kg/cm}^2$  and a Poisson ratio of 0.3 are assumed for the core plate and the BRM components. A nonlinear combined isotropic-kinematic hardening rule is employed to reproduce the inelastic material property and therefore an accurate cyclic behavior. The selection of the hardening parameters is based on Coupon test results, as observed in experiments conducted by Tremblay et al. (2006). In addition, the initial kinematic hardening modulus,  $C$ , and the rate factor,  $\gamma$ , are assumed to be  $8 \times 10^4 \text{ Kg/cm}^2$  and 75, respectively (Korczekwa et al. 2009). For isotropic hardening, a maximum change in yield stress of  $Q_\infty = 1100 \text{ Kg/cm}^2$  and a rate factor of  $b = 4$  are adopted. An initial imperfection of 0.2 cm (i.e.,  $L/1000$ ) is considered in both the core plate and the BRM member.

**Table 1.** The proposed BRB models' specifications

No.	Model Name	BRM section dimensions (cm)	core dimensions (cm)	gap (cm)	Unbonding Thickness(cm)	$\mu$
1	S1g0c1	BOX ( $5 \times 5 \times 0.4$ ) + 2 Face plate ( $4.5 \times 0.5$ )	Plate $10 \times 1$	0.0	-	0.1
2	S1g1c1	BOX ( $5 \times 5 \times 0.4$ ) + 2 Face plate ( $4.5 \times 0.5$ )	Plate $10 \times 1$	0.1	-	0.1
3	S1u1	BOX ( $5 \times 5 \times 0.4$ ) + 2 Face plate ( $4.5 \times 0.5$ )	Plate $10 \times 1$	-	0.1	0.075
4	S1g0c2	BOX ( $5 \times 5 \times 0.4$ ) + 2 Face plate ( $4.5 \times 0.5$ )	Plate $10 \times 1$	0.0	-	0.3
5	S2g0c1	UNP 65 + 2 Face plate ( $3.75 \times 0.5$ )	Plate $10 \times 1$	0.0	-	0.1
6	S2g0c2	UNP 65 + 2 Face plate ( $3.75 \times 0.5$ )	Plate $10 \times 1$	0.0	-	0.3
7	S1g1c2	BOX ( $5 \times 5 \times 0.4$ ) + 2 Face plate ( $4.5 \times 0.5$ )	Plate $10 \times 1$	0.1	-	0.3
8	S2g1c1	UNP 65 + 2 Face plate ( $3.75 \times 0.5$ )	Plate $10 \times 1$	0.1	-	0.1
9	S2g1c2	UNP 65 + 2 Face plate ( $3.75 \times 0.5$ )	Plate $10 \times 1$	0.1	-	0.3
10	S1g5c1	BOX ( $5 \times 5 \times 0.4$ ) + 2 Face plate ( $4.5 \times 0.5$ )	Plate $10 \times 1$	0.5	-	0.1
11	S1u2	BOX ( $5 \times 5 \times 0.4$ ) + 2 Face plate ( $4.5 \times 0.5$ )	Plate $10 \times 1$	-	0.2	0.075
12	S1u5	BOX ( $5 \times 5 \times 0.4$ ) + 2 Face plate ( $4.5 \times 0.5$ )	Plate $10 \times 1$	-	0.5	0.075

Because of low rigidity and stiffness, the finite element models do not consider the effect of unbonding material. Previous studies conducted by Kasai et al. (2007) confirm the validation of such an assumption. Therefore, the thickness of unbonding material is assumed as an air gap. In addition, a friction coefficient of 0.075 is adopted for the contact surface of the core and the BRM based on previous studies (Usami et al. 2006).

The axial deformation is blocked at one end of bracing with a pinned connection. Axial displacements are enforced at the other end following the cyclic quasi static protocol suggested by AISC seismic provisions for BRBs as follows: 2 cycles at  $\pm \Delta_y$ , 2 cycles at  $\pm 0.5 \Delta_{bm}$ , 2 cycles at  $\pm \Delta_{bm}$ , 2 cycles at  $\pm 1.5 \Delta_{bm}$ , and 2 cycles at  $\pm 2 \Delta_{bm}$ , where  $\Delta_y$  is the displacement that corresponds to the yielding of the core, and  $\Delta_{bm}$  is the axial deformation of the brace corresponding to the design story drift. Based on the previous studies by Tremblay et al. (2006), the peak strain amplitude in full-length BRBs typically falls in the range of 0.01 to 0.02 for common structural applications, and peak deformation in the majority of

past test programs have been limited to that range (Watanabe et al. 2003). In this study,  $\Delta_{bm}$  is set to 2 cm, which corresponds to the axial strain of 1% in the core, and the core yielding displacement,  $\Delta_y$ , is calculated as 0.37 cm based on the material characteristics. Therefore, the ultimate axial displacement demand of the brace during cyclic loading will be  $2\Delta_{bm}=4$  cm, which corresponds to a core strain of 2%. Therefore, the adopted value for the peak strain demand of the core plate seems reasonable. A finite element representation of the proposed BRBs is illustrated in Fig. 2.

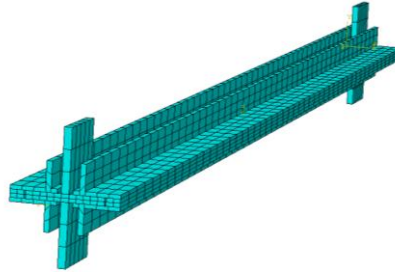


**Figure 2.** Finite element representation of a proposed BRB

### 3. RESULTS AND DISCUSSIONS

#### 3.1 Effect of interface detail of BRB on local buckling behavior of the brace

As mentioned previously, three types of interface details are considered in this part. Hysteretic responses in the BRBs are well predicted by the finite element models in both elastic and nonlinear ranges. Fig. 3a shows the normalized hysteretic response curves of models S1g0c1, S1g1c1, and S1u1. Axial force-displacement curves of the models are captured from a point at the brace end. This point is located in a region that essentially remains elastic, because stiffener plates are provided in this region to prevent local buckling in the brace end. Therefore, the captured force-displacement relation may not be a representation of the true stress distribution of the core during cyclic loading, although the curves properly describe the local undulations due to core local buckling.

The normalized (respect to the yield displacement and the yield force of the core) axial force-displacement curves shown in Fig. 3a point out the stable behavior in all of the models. However, some local instability is observed in models S1g1c1 and S1u1 due to local buckling of the core plate about weak axis under compression. It is clear that in model S1g0c1 with the direct contact of the core plate and the BRM, local buckling of the core plate does not occur about the core weak axis, however a high frictional response is resulted at the interface due not to providing gap. In addition, local buckling of the core plate about strong axis of the core is observed due to the presence of the gap employed through the core width in model S1g0c1.

The compression strength and strain hardening adjustment factors,  $\beta$  and  $\omega$ , for the BRB models are represented in Table 2. The highest value of  $\beta$  factor belongs to model S1g0c1 with direct contact of the core and the BRM, and the minimum value belongs to model S1u1 with unbonding material at the core and the encasing interface, as shown in Table 2. However, the amount of the factor  $\beta$  in the model S1u1 is not significantly smaller than that in the model S1g1c1. Because of the employing the unbonding agent with the thickness of 1mm on both sides of the core plate, excessive local buckling of the core plate is resulted, which causes the higher frictional response between the core plate and the BRM in model S1u1. Instead, the friction coefficient in model S1u1 is smaller than that in model S1g1c1, which causes to keep the frictional response and dissipated energy by friction closely near together in models S1g1c1 and S1u1.

**Table 2.** Compression strength and strain hardening adjustment factors of the models in part 1

No.	Model name	$\varepsilon$ (core) =2%	
		$\omega$	$\beta$
1	S4g0c1	0.97	1.19
2	S4g1c1	0.91	1.04
3	S4u1	0.92	1.00

Based on the results, all three types of interface configurations are well capable of the generation of a stable hysteretic behavior in BRBs. The Results show that local buckling of the core plate can be reduced by using a direct contact between the core and the encasing. In any way, this type of interface detail generates high frictional forces at the core and the encasing interface, which results in greater amounts of  $\beta$  factors. Moreover, employing unbonding material between the core and the BRM can significantly decrease the frictional forces developed at the interface, however local buckling of the core may not be prevented due to inadequate lateral stiffness of the unbonding material.

The results show that the core axial stress distribution in model S1g0c1 is more uniform in comparison to models S1g1c1 and S1u1, because the local buckling of the core plate is inhabited in model S1g0c1 through a direct contact of the core and the BRM. Local buckling of the core plate in models S1g1c1 and S1u1 occurs due to the presence of gap and low rigidity of the unbonding material, respectively. Therefore, a non-uniform axial stress distribution in the core plate is observed due to the effect of bending stresses at the buckled regions. Fig. 3b shows the frictional dissipated energy curves in models S1g0c1, S1g1c1, and S1u1. As shown in Fig. 3b, the frictional dissipated energy in model S1g0c1 is significantly greater in comparison to the other models due to the direct contact of the core plate and the encasing. In addition, the dissipated energy in model S1g1c1 is smaller than that in model S1u1 despite of a smaller value of friction coefficient in model S1u1, i.e., 0.075, because the unbonding material employed on both sides of the core plate through the core thickness, which is modeled as a gap in both sides of the core in the finite element models, causes the core plate to undergo larger local buckling amplitudes under compression. The excessive local buckling causes to increase in the contact points of the core plate and the encasing, which results in the development of excessive frictional forces at the interface.

Local buckling of the core plate should be controlled in order to minimize the frictional response between the core plate and the BRM and keep the uniformity of the core axial force demand. Based on the results of this study, a minimum amount of gap or unbonding material thickness such as 1mm does not significantly affect the uniformity of axial stress demand distribution of the core plate, despite of some local instabilities and the stress concentration at peak amplitudes of the buckles in the core plate. In the other words, if the ratio of the gap size or the unbonding material thickness to the thickness of the core plate is small enough, local buckling amplitudes will be kept limited and the core axial force demand will be closely uniform. It should be stated that the BRB models considered in this part have a  $P_e/P_y$  ratio greater than 2.5, which guarantees the global buckling prevention of the entire BRB due to adequate rigidity and stiffness of the encasing member. The overall buckling prevention condition of  $P_e/P_y \geq 1$ , where  $P_e$  and  $P_y$  denote the Euler buckling load and the yield load of the core respectively, exists in the literature (Watanabe et al. 2003).

Because the costs of using an unbonding material is less when compared to the total costs of manufacturing an all-steel BRB, it is strongly recommended that such a material is used at the interface to achieve a lower amount of factor  $\beta$  and minimize the frictional response and force demands in the brace adjacent elements such as end connections, subsequently. It is clear that the magnitude of factor  $\beta$  is solely dependent on the interface detail of a BRB. In actual design, a gap through width of the core plate should be provided to allow for free lateral expansion of the core plate under compression. Thus, among three types of interface configurations of all steel BRBs, using unbonding material with a proper thickness, e.g., 1mm at the interface is suggested for practical applications. Such a detail for all-steel BRBs minimizes the frictional response developed at the core and the encasing interface and provides a closely uniform axial force demand throughout the core plate.

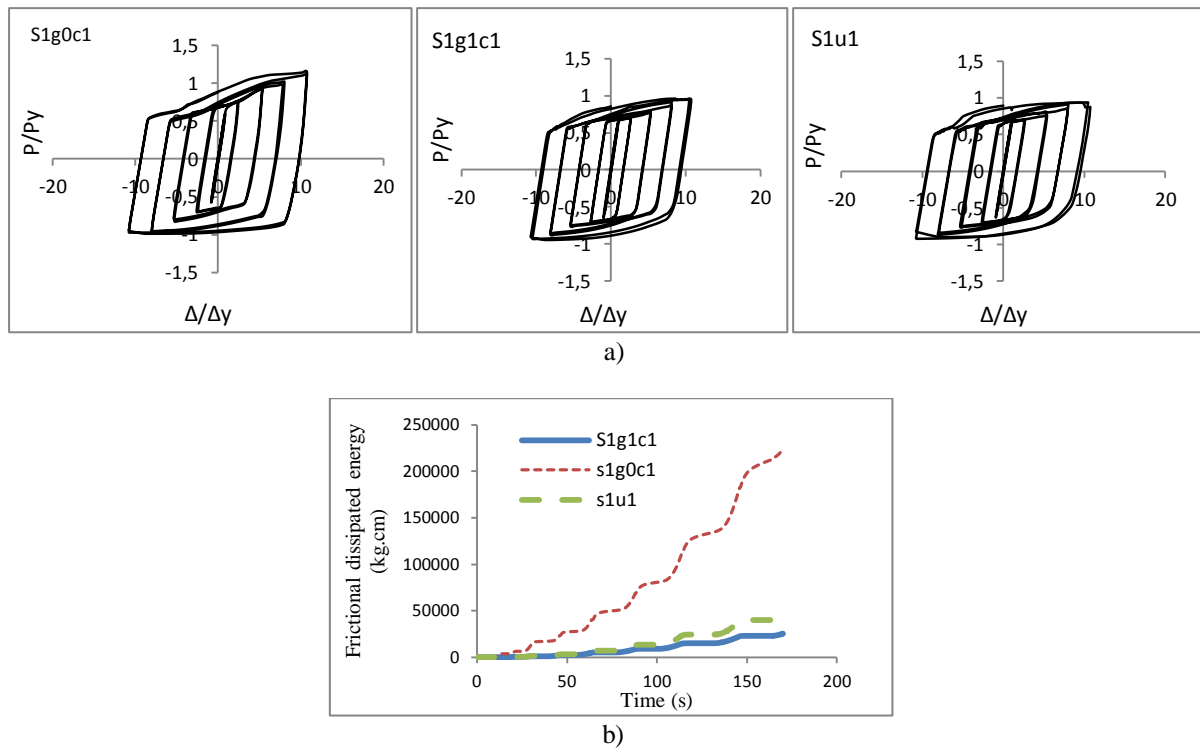


**Fig. 3.** a) Hysteretic responses of models S1g0c1, S1g1c1, and S1u1;  
b) Frictional dissipated energy of the models

### 3.2. Effect of the magnitude of friction coefficient at the interface on buckling pattern of the brace

The effect of the magnitude of friction coefficient of the core and the encasing contact surface on local buckling behavior of all-steel BRBs have been numerically studied in this part. Eight finite element analyses have been performed on the proposed BRBs consist of different amounts of gap sizes and friction coefficients at the interface.. The friction coefficients of 0.1 and 0.3 assumed for the models in Table 1 correspond with a greasy and a smooth steel-to-steel surface contact of the core plate and the BRM member, respectively. Hysteretic response curves of the models are represented in Fig. 4.

Fig. 4 reveals that the buckling pattern of the BRB models depend on the magnitude of the friction coefficient at the interface. For example, the models with the friction coefficient of 0.1 experience only the local buckling of the core plate under compression, which corresponds with small local undulations in the hysteretic curves. However, there is a high potential of global buckling of the entire brace in the models with friction coefficient of 0.3, which corresponds with the sudden fall in the brace strength on the hysteretic response curves. Table 3 summarizes the compression strength adjustment factors and buckling patterns of the models.

**Table 3.** Analyses results of the proposed BRB models in part 2

No.	Model name	$\beta$	$\omega$	Buckling pattern
1	S1g0c1	1.19	0.97	No
2	S1g0c2	-	1.01	Global
3	S2g0c1	1.01	0.95	No
4	S2g0c2	-	0.93	Global
5	S1g1c1	1.04	0.91	Local
6	S1g1c2	1.28	0.88	Local
7	S2g1c1	1.01	0.93	Local
8	S2g1c2	-	0.89	Global

Based on the results, buckling pattern of a BRB appears to be dependent on the interface detail, especially the magnitude of the friction coefficient between the core and the encasing member.

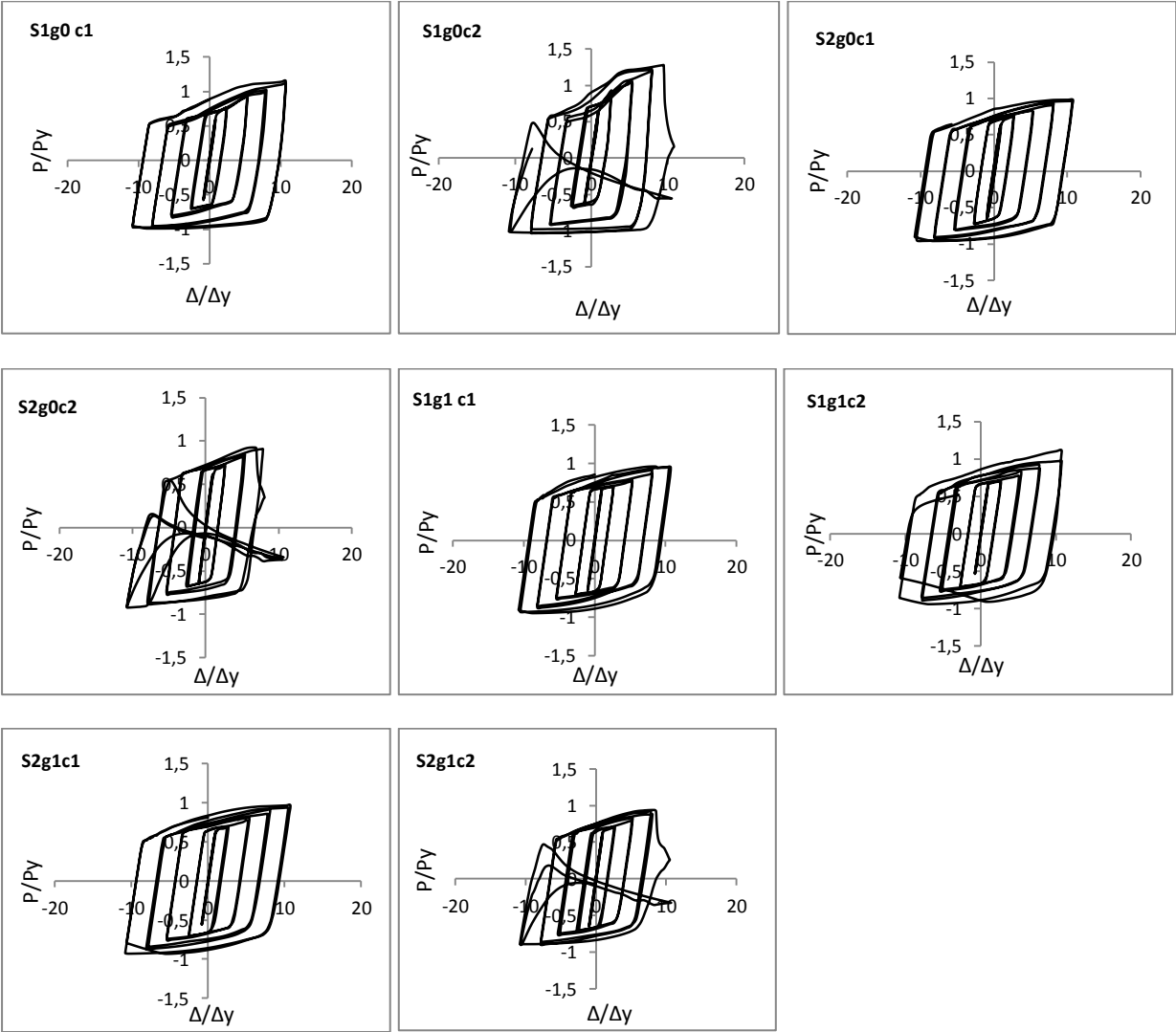


Figure 4. Hysteretic responses of the proposed BRBs

Table 3 shows that models S1g0c1 and S2g0c1 with the friction coefficient of 0.1 do not experience global buckling under compression. However, in models S1g0c2 and S2g0c2 with the same gap sizes and the friction coefficients of 0.3, global buckling occurs during cyclic loading of the brace. In addition, models S1g1c1, S1g1c2, and S2g1c1 do not endure global buckling; however, in the model S2g1c2, global buckling occurs before the brace reaches the target axial displacement demand. It should be note that  $P_e/P_y$  ratios in all of the models are greater than 1.5. Previous studies showed that a minimum ratio of  $P_e/P_y = 1$  is mandatory for the prevention of overall buckling in all-steel BRBs. In the mentioned studies, the amount of friction coefficient between core and BRM was not considered as an effective parameter on global response of the brace (Watanabe et al. 2003). Therefore, an extensive effort is required to investigate the global buckling behavior of BRBs considering the effect of the interface frictional response.

When the magnitude of the friction coefficient between the core and the BRM contact is high, the slippage of the core plate inside the encasing does not occur freely under compression, which causes to the development of excessive shear forces between the locally buckled regions of the core plate and the encasing member. The developed large shear forces at the interface bring about the buckled regions of

the core to be closely constrained to the encasing at the contact surfaces. Therefore, the core plate and the encasing member may act as an integrated member at the contacted regions like a member with intermittent welded connections, which causes the lateral bending of the entire BRB due to the increase in compression displacement of the brace instead of free slippage and full axial plastic deformation of the core. In addition, the developed shear forces at the interface enhance the transferred axial loads in the BRM containing initial imperfections, which may cause the flexural buckling of the entire brace under compression. Therefore, choosing a proper interface detail in all-steel BRBs is more important to obtain a desirable performance. In the other words, the interface detail can significantly change the buckling pattern and the stress distribution of the core plate in a BRB.

#### 4. CONCLUSIONS

One of the key requirements for the desirable mechanical behavior of all-steel buckling restrained braces under severe earthquake loading is to control the local buckling of the core plate. Various details may be considered for the interface between the core plate and the buckling restraining mechanism in practice, consist of the direct contact of the core and the encasing, using gap, or employing unbonding material at the interface. In this paper, finite element analyses of the proposed all-steel BRBs are performed to investigate the effect of the interface detail on local buckling behavior of the brace member. Moreover, the effect of the magnitude of friction coefficient of the contact between the core and the BRM on local buckling behavior is investigated through the finite element analysis method. The main out comings of this study can be summarized as follows:

- 1- Among three types of interface details of all-steel BRBs consist of the direct contact, using gap, and using unbonding material, the application of unbonding material with a proper thickness is suggested as the most appropriate detail, where it can minimize the frictional response, control the local buckling of the core, and produce a stable hysteretic behavior in all-steel BRBs.
- 2- The increase in the magnitude of friction coefficient of the core and the BRM contact causes the increase in frictional response and the compression strength adjustment factor. In addition, the buckling pattern of a BRB may depend on the magnitude of friction coefficient. When the magnitude of friction coefficient between the core and the BRM contact is high, the slippage of the core plate inside the encasing does not occur freely under compression, which causes the development of excessive shear forces and lateral bending of the entire BRB during the increase in compression displacement of the brace. In addition, the developed shear forces at the interface enhance the transferred axial loads in the BRM containing initial imperfections, which may cause the flexural buckling of the entire brace.

#### REFERENCES

- ABAQUS. Standard user's manual version 6.3. Pawtucket, RI: Hibbitt, Karlsson & Sorensen, Inc., 2003.
- AISC (American Institute of Steel Construction). Seismic provisions for structural steel buildings, Chicago, IL 2005.
- Black, C.J., Makris, N., and Aiken, I.D. (2002). Component Testing, Stability Analysis, and Characterization of Buckling Restrained Braced Frames. Report No. *PEER 2002/08*, Univ. of California, Berkeley, CA.
- Clark, P., Aiken, I., Kasai, K., Ko, E., Kimura, I. (1999). Design procedures for buildings incorporating hysteretic damping devices. In *Proceeding of 69th annual convention*, p. 355-371.
- Chou, C., Chen, S. (2010). Subassemblage tests and finite element analyses of sandwiched buckling restrained braces. *Engineering Structures*, **32**: 2108-2121.
- Eryasar, M., Topkaya, C. (2010). An experimental study on steel-encased buckling restrained brace hysteretic damper. *Journal of Earthquake Engineering and Structural Dynamics*; **39**: 561-581.
- Fahnestock, L.A., Sause, R., Ricles, J.M. (2007). Seismic response and performance of buckling-restrained braced frames. *Journal of the Structural Engineering*, **133**(9): 1195-204.
- Inoue, K., Sawaizumi, S., Higashibata, Y. 2001. Stiffening requirements for unbonded braces encased in concrete panels. *ASCE, Journal of structural engineering*, **127**(6): 712-719.
- Kato, M., Usami, T., and Kasai, A. (2002). A numerical study on cyclic elasto-plastic behavior of buckling-restraining brace members. *Journal of structural engineering*, **48A**: 641-648.

- Kinoshita, T., Koetaka, Y., Inoue, K., and Iitani, K. (2007). Criteria of buckling-restrained braces to prevent out-of-plane buckling. *Journal of Structure and Construction Engineering*, **621**: 141-8.
- Kasai, A., Usami, T., and Watanabe, N. (2007). Whole buckling behavior of buckling restrained brace members. *ECCOMAS Thematic conference on computational methods in structural dynamics and earthquake engineering*, Greece.
- Korzekwa, A., and Tremblay, R. (2009). Numerical simulation of the cyclic inelastic behavior of buckling restrained braces. Taylor & Francis Group, London, ISBN 978-0-415-56326-0.
- Matsui, R., Takeuchi, T., Hajjar, JF., Nishimoto, K., and Aiken, I. (2008). Local Buckling Restraint Condition for Core Plates in Buckling-Restrained Braces. *In Proceeding of 14th World Conference on Earthquake Eng.* Beijing, China, Paper No.05-05-0055.
- Nakamura, H., Maeda, Y., Sasaki, T., Wada, A., Takeuchi, T., Nakata, Y., and Iwata, M. (2000). Fatigue properties of practical-scale unbounded braces. Nippon Steel technical report, No.82, 51-57.
- Ma, N., Wu, Z., Li, h., Ou, j., and Yang, w. (2008). Full scale test of all-steel buckling restrained braces. *In proceeding of 14th world conference on earthquake engineering*, Beijing, China, paper No. 11-0208.
- Qiang, X. (2005). State of the art of buckling-restrained braces in Asia. *Journal of Constructional Steel Research*; **61**:727-48.
- Sabelli, R., Mahin, S., Chang, C. (2003). Seismic demands on steel braced frame buildings with buckling-restrained braces. *Journal of Engineering Structures*; **5**: 655-66.
- Tembata, H., Koetaka, Y., Inoue, K. (2004). Out-of-plane buckling load of buckling restrained braces including brace joints. *Journal of Structure and Construction Engineering*, **581**: 127-134.
- Takeuchi, T., Suzuki, K., Marukawa, T., Kimura, Y., Ogawa, T., and Sugiyama, T. (2005). Performance of compressive tube members with buckling restrained composed of mortar in-filled steel tube. *Journal of Structure and Construction Engineering*, **590**: 71-8.
- Tremblay, R., Bolduc, P., Neville, R, and DeVall, R. (2006). Seismic testing and performance of buckling restrained bracing systems. *Canadian journal of civil engineering*, **33(1)**: 183-198.
- Uang, C., Nakashima, M. (2004). Steel buckling restrained braced frames, Earthquake engineering from engineering seismology to performance based engineering. CRC press: Boca Raton.
- Usami, T. (2006). Guidelines for Seismic and Damage Control Design of Steel Bridges. Japanese Society of Steel Construction , Gihodo-Shuppan, Tokyo, Japan.
- Watanabe, N., Kato, M., Usami, T., and Kasai, A. (2003). Experimental study on cyclic elasto-plastic behavior of buckling-restraining braces. *Journal of Earthquake Engineering*, Paper No.133.
- Wei, Ch., and Tsai, K. (2008). Local buckling of bucking restrained braces. *In proceeding of 14th world conference on earthquake engineering*, Beijing, China.
- Xie, Q. (2005). State of the art of buckling restrained braces in Asia. *Journal of constructional steel researches*, **61**:727-748.